Historical variability and feedbacks among land cover, stream power, and channel geometry along the lower Canadian River floodplain in Oklahoma

Jason P. Julian,[1]* Richard E. Thomas,[1] Sayed Moursi,[2] Bruce W. Hoagland[1] and Aondover Tarhule[1]
[1] University of Oklahoma, Department of Geography & Environmental Sustainability, Norman, OK, USA
[2] Fayoum University, Department of Geography, Fayoum City, Egypt

*Correspondence to: Jason P. Julian, University of Oklahoma, Department of Geography & Environmental Sustainability, Norman, OK, USA. E-mail: jjulian@ou.edu

ABSTRACT: In 1820, the lower Canadian River meandered through a densely forested floodplain. By 1898, most of the floodplain had been cleared for agriculture and changes in channel geometry and specific stream power followed, particularly channel widening and straightening with a lower potential specific stream power. In 1964, a large upstream hydropower dam was constructed, which changed the flow regime in the lower Canadian River and consequently the channel geometry. Without destructive overbank floods, the channel narrowed rapidly and considerably due to encroachment by floodplain vegetation. The lower Canadian River, which was once a highly dynamic floodplain-river system, has now been transformed into a relatively static river channel. These changes over the past 200 years have not been linear or independent. In this article, we use a variety of data sources to assess these historical changes along the lower Canadian River floodplain and identify feedbacks among floodplain cultivation, dam construction, specific stream power, and channel width, slope, and sinuosity. Finally, we combine the results of our study with others in the region to present a biogeomorphic response model for large Great Plains rivers that characterizes channel width changes in response to climate variability and anthropogenic disturbances. Copyright © 2011 John Wiley & Sons, Ltd.

KEYWORDS: historical range of variability; biogeomorphic feedbacks; fluvial geomorphology; riparian vegetation; agricultural land use; Southern Great Plains

Introduction

Floodplains, especially along large rivers, are one of the most productive and valuable environments on earth, providing abundant ecosystem and human services (Costanza *et al.*, 1997; Tockner and Stanford, 2002). These high-quality environments are created by high flow variability, dynamic river channels, and complex vegetation patterns (Junk *et al.*, 1989). The integrity of floodplains therefore depends on the maintenance of these three factors. Because of the interdependency among streamflow, channel geometry and floodplain vegetation, any change in one variable will likely lead to a change in one or both of the other variables, and possibly a feedback to the original variable (Schumm and Lichty, 1965; Gregory *et al.*, 1991). These feedbacks make it difficult to assign cause-and-effect in channel processes. However, by using a long period of empirical data, we can assess patterns and then infer process from these patterns. This approach is particularly useful when trying to understand drivers and impacts of the historical range of variability of large river-floodplain systems.

   Primarily due to extreme climate variability, the rivers and floodplains of the Great Plains, USA are some of the most dynamic in the world (Matthews *et al.*, 2005; Dort, 2009). Yet there exists a huge gap in our knowledge of these Great Plains rivers, both geographically and historically (Graf, 2001). The

historical studies that have been conducted in this region have shown that under 'natural' conditions channel geometry (width and planform) changes gradually in response to variable flow conditions, and sometimes drastically during large floods (Friedman *et al.*, 1996; Curtis and Whitney, 2003; Dort, 2009). Most Great Plains rivers, however, have experienced considerable flow reductions from irrigation, diversions, lowering water tables, and upstream impoundments (Graf, 2001). The consequence has been narrowing of most of the region's large rivers, largely due to floodplain vegetation encroachment in the active channel (Martin and Johnson, 1987; VanLooy and Martin, 2005; Joeckel and Henebry, 2008). Channel curvature and migration patterns have also been altered by these landscape changes (Friedman *et al.*, 1998).

   While many studies have analyzed adjustments to channel width and planform in response to hydrological changes, only recently has the influence of floodplain land cover on erosion rates for large rivers been evaluated (e.g. Micheli *et al.*, 2004). This study and others have shown that forested streambanks are considerably more resistant to erosion than deforested streambanks because of the increased soil strength provided by roots and the decreased applied shear stresses due to increased surface roughness (Thorne, 1990). From their analyses of a central reach of the Sacramento River, Micheli *et al.* (2004) found that agricultural floodplains were 80–150% more erodible

than forested floodplains. Similarly, Zaimes *et al.* (2004) found that erosion rates along a stream in central Iowa were 108% higher for pastoral banks and 173% higher for cultivated banks, when compared to forested banks. With all the land-cover changes that have occurred in the floodplains of the Great Plains over the past century, particularly large increases in agricultural land use (Tockner and Stanford, 2002; Jones *et al.*, 2010), there have likely been feedbacks with channel geometry and flow characteristics. In the following discussion we evaluate the historical range of variability and feedbacks among floodplain land cover, channel geometry, and stream power for a river reach in the Southern Great Plains that has experienced considerable land-cover changes over the past two centuries and has been impacted by an upstream dam over the past five decades.

Methods

Study area

The Canadian River begins in the southern Rocky Mountains of New Mexico and flows 1644 km across the Great Plains of Texas and Oklahoma before emptying into the Arkansas River (Figure 1). The upper basin of the Canadian River is located in a warm arid region where most of its precipitation (< 40 cm/yr) is lost to evapotranspiration. Precipitation increases eastward, with 120 cm/yr at the basin outlet. Land cover for the 122 070-km^2 drainage area of the Canadian River in 2006 was 52% Grassland, 16% Agriculture, 15% Shrubland, 12% Forest, 4% Urban, and 1% Water. Except for the coniferous forests of the southern Rocky Mountains, forest cover increases eastward across the basin, with our study reach being located in predominantly oak-hickory forests. The Canadian floodplain consists of Holocene-age alluvial deposits of mostly sand, which had been aggrading for the past two centuries (pre-dam) due to large floods with high bedload (Curtis and Whitney, 2003).

Our study reach, lower Canadian River floodplain (LCRF; LCR, lower Canadian River), begins 2·5 km downstream of the Lake Eufaula Dam (latitude, 35·296; longitude, –95·333), which minimizes immediate hydraulic and 'hungry water' effects of the dam on channel width. Our study reach ends ~10 km

upstream of Lake Kerr (latitude, 35·406, longitude, –95·087), which minimizes backwater effects from the lake. Lake Eufaula Dam was completed in February 1964, with reservoir filling beginning in August 1963. It took about four years for the reservoir to reach its normal storage of 2855 km^3. Maximum storage capacity behind the 34-m high dam is 4718 m^3. The dam is used for recreation, flood control, and hydropower, with this last function dictating the timing, magnitude, and ramping rate of daily discharges.

Vegetation in LCRF is and was distributed in a mosaic (Hefley, 1937; Ware and Penfound, 1949; Hoagland, 2000). Active channel margins and in-stream bars are dominated by cottonwood (*Populus deltoides*) and sand bar willow (*Salix exigua*), with a few sparse occurrences of tamarisk (*Tamarix* spp.). Sand plum (*Prunus angustifolia*) and switchgrass (*Panicum virgatum*) are present on large sand deposits and adjacent terraces. Black willow (*Salix nigra*) and cottonwood (*Populus deltoides*) stands, interspersed with boxelder (*Acer negundo*), American sycamore (*Platanus occidentalis*), and silver maple (*Acer saccharinum*), predominate in portions of the floodplain that experience early spring flooding with a short hydroperiod. Forested areas least exposed to flooding are composed of green ash (*Fraxinus pennsylvanica*), slippery or red elm (*Ulmus rubra*), and hackberry (*Celtis occidentalis*) or sugarberry (*Celtis laevigata*). Mesic terraces consist of an assortment of bur oak (*Quercus macrocarpa*), shumard oak (*Quercus shumardii*), chinkapin oak (*Quercus muehlenbergii*), bitternut hickory (*Carya cordiformis*), pecan (*Carya illinoinensis*), black walnut (*Juglans nigra*), and increasingly eastern red cedar (*Juniperus virginiana*). Croplands, mostly corn and soybeans, and pasture grasses, likely bermudagrass (*Cynodon dactylon*), crown grass (*Paspalum* spp.), and fescue (*Schedonorus phoenix*), now occupy large areas of the floodplain.

The LCRF before European settlement was largely forested (James, 1905), with sparse, localized farming beginning in the region about 1500 yr BP (Matthews *et al.*, 2005). In the 1830s, the Cherokee and Choctaw tribes were forced to settle in Eastern Oklahoma north and south of LCR, respectively. The floodplain did not experience widespread agriculture until the mid-nineteenth century when a military encampment and trading post were established at the current location of Whitefield, Oklahoma. It was not until after 1898 with the passage of the Curtis Act that large portions of LCRF was converted to large-scale agriculture.
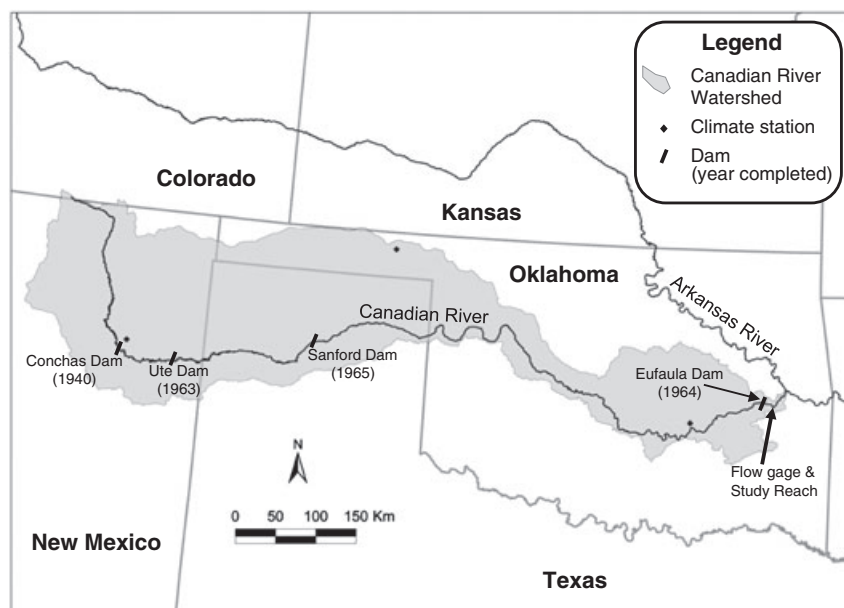

Figure 1. Canadian River watershed in south-central United States. The study area is the lower Canadian River floodplain (LCRF) between Eufaula Dam and the confluence with the Arkansas River.

Land cover mapping

The modern floodplain of our study area was delineated using a 30-m digital elevation model (DEM) in combination with flood stage history and aerial photographs, which resulted in a maximum floodplain elevation 160 m above mean sea level. Land cover mapping of this floodplain area was performed using a variety of sources. Historical aerial photographs, after georeferencing, were used for mapping land cover for the following years: 1939, 1941, 1952, 1958, 1964, 1972, 1980, 1984, 1990, and 1995. In two cases, we had to replace missing photographs with ones from the following year: one-quarter of the 1980 photographs is from March 16, 1981, and two-fifths of the 1990 photographs are from February 7, 1991 Oklahoma. Digital Orthophoto Quarter Quads (DOQQs) from the National Agriculture Imagery Program (NAIP) were used for mapping land cover for 2003 and 2008. For 1898, we used the survey plats and field notes from the General Land Office (GLO), again georeferencing before digitizing. The GLO plats have been successfully used in numerous studies to analyze land cover (Schulte and Mladenoff, 2001; Whitney and DeCant, 2001). While GLO records have potential errors, we have confidence in the land cover and channel geometry depicted on the plats we used because our study reach was an important navigation corridor that also formed the boundary between two Indian nations, and thus our data was extracted from plat boundaries. In order to create a land cover map for 1820, we relied on the detailed account of S.H. Long's expedition along our study reach in 1820 (James, 1905). Channel locations for 1820 were approximated using meander scars from early aerial photographs and using similar channel geometry as 1898.

All imagery and maps were reviewed at a scale of 1:10 000 to digitize land cover for each year using the Anderson *et al.* (1976) Level II classification system, with Cropland and Pasture segregated. To nullify seasonal effects on land cover (rotational grazing, groundwater levels), we used the following land use groups (inclusive Level II categories): Forest (Deciduous Forest Land and Forested Wetlands), Grassland (Herbaceous Rangeland, Pasture, and Non-forested Wetlands), Cropland; and Water/Sand. The active channel was delineated according to Osterkamp and Hedman (1977), which is the area of channel being shaped by prevailing discharges and is marked by the lower limit of permanent vegetation, large trees in this case. Soil composition, measured as weighted average silt-clay percentage (SC%) of the entire soil depth, of the floodplain was derived from the Natural Resources Conservation Service's Soil Survey Geographic Database (SSURGO), where surveys occurred in 2003.

In order to contextualize floodplain changes in land cover within a broader and socio-economic timeline, we used US agricultural censuses (for the years that closely coincided with our historical imagery) to document temporal changes in total cropland area for the two counties (Muskogee and Haskell) that surround our study reach. Because the state of Oklahoma was not established until 1907, we used data from Watkins (2007; Haskell County only) to calculate cropland area in 1898. This data was derived from GLO surveys and notes.

Hydrologic analyses

Precipitation of the watershed was characterized with three fairly equally spaced US Historical Climate Network (USHCN) stations (Figure 1) representing the western, central, and eastern third of the basin respectively (IDs: 290858, 340593, 344235). These three stations were chosen based on the span (1890s to 2008) and completeness of their records. Any missing records were replaced by values from the next nearest USHCN station, usually within 60 km. We also used monthly East-Central Oklahoma regional data (1895–2008) from the National Climatic Data Center (NCDC, 2011) for comparison and validation. Daily discharge (Q) for 1938 to 2008 was obtained from the US Geological Survey gage near Whitefield, Oklahoma (USGS 07245000), which is located in the center of the study reach. From the portion of the time-series not influenced by Lake Eufaula Dam (1938–1963), we calculated the mean annual flood, which has a recurrence interval of 2·33 yr ($Q_{2.33}$) and is commonly used as a 'dominant' discharge (i.e. large enough to shape the channel, yet with a recurrence interval frequent enough to maintain the active channel geometry).

In order to characterize hydrologic regime beyond the pre-dam gaged record of 1938 to 1963, we investigated rainfall–runoff relationships during this period to find which metric of rainfall correlated best with flood discharges. First we compared flood event peaks with center of mass of rainfall events, which revealed that mean [± standard deviation (SD)] travel time for flood waves was 4 ± 1 days for the upper station, 3 ± 1 days for the central station, and 1 ± 1 days for the lower station. Using these travel times to match rainfall events with the 25 largest flood events, we found that individual flow events were not significantly related to rainfall magnitude of either the upper ($r = 0.20$, $p = 0.33$) or central ($r = 0.09$, $p = 0.65$) stations, likely due to the low runoff potential and high transmission losses in the upper and central portions of the Canadian River Basin (Matthews *et al.*, 2005). The lower station, however, was a significant predictor of peak discharge ($r = 0.65$, $p < 0.001$). Upon further investigation, we found the three-day total precipitation for the lower station to be the best bivariate predictor of Q ($r = 0.71$, $p < 0.001$). This metric was useful for assessing long-term precipitation and runoff trends. In particular, we constituted a new time-series of the ratio of runoff (Q) to the three-day precipitation (P_{3d}) and tested for temporal trends using simple linear regression analysis. The 110-yr precipitation record was also analyzed for temporal trends and stationarity using a Mann–Kendall test.

Channel pattern and dimensions are dictated by slope–discharge relationships, especially for large rivers in sandy alluvium (Nanson and Croke, 1992). Thus, we used specific stream power ($\omega = \gamma QS/w_{ac}$) in W/m² as a channel change driver, where γ is the specific weight of water (9800 N/m³), Q is river discharge in m³/s, S is water surface slope (Δ elevation/stream length), and w_{ac} is water surface width of the active channel in meters. Change in elevation over the reach was derived from the DEM. Stream length and w_{ac} were derived from the aerial photographs for 1938 to 2008 and from the survey plats for 1898. The $Q_{2.33}$ represents the threshold above which we compared ω to channel geometry. Given that channel erosion and riparian vegetation patterns are driven by numerous processes over various timescales (Hooke, 1979; Thorne, 1982; Hupp and Osterkamp, 1996), we assessed the event peak, magnitude, duration, and variability of ω to evaluate which of these four properties was most strongly correlated to channel changes (sensu Julian and Torres, 2006). These four properties are defined as: Event peak (in W/m²) = ω_{max}; Magnitude (in W/m²) = $\Sigma \omega$ when $Q > Q_{2.33}$; Duration (in days) = time in which $Q > Q_{2.33}$; and Variability (#) = number of individual flood events $> Q_{2.33}$.

Results

Precipitation and discharge

Precipitation was variable over the 110-yr study period with several droughts and numerous large storms (Figure 2), which is characteristic of the Great Plains (Matthews *et al.*, 2005;
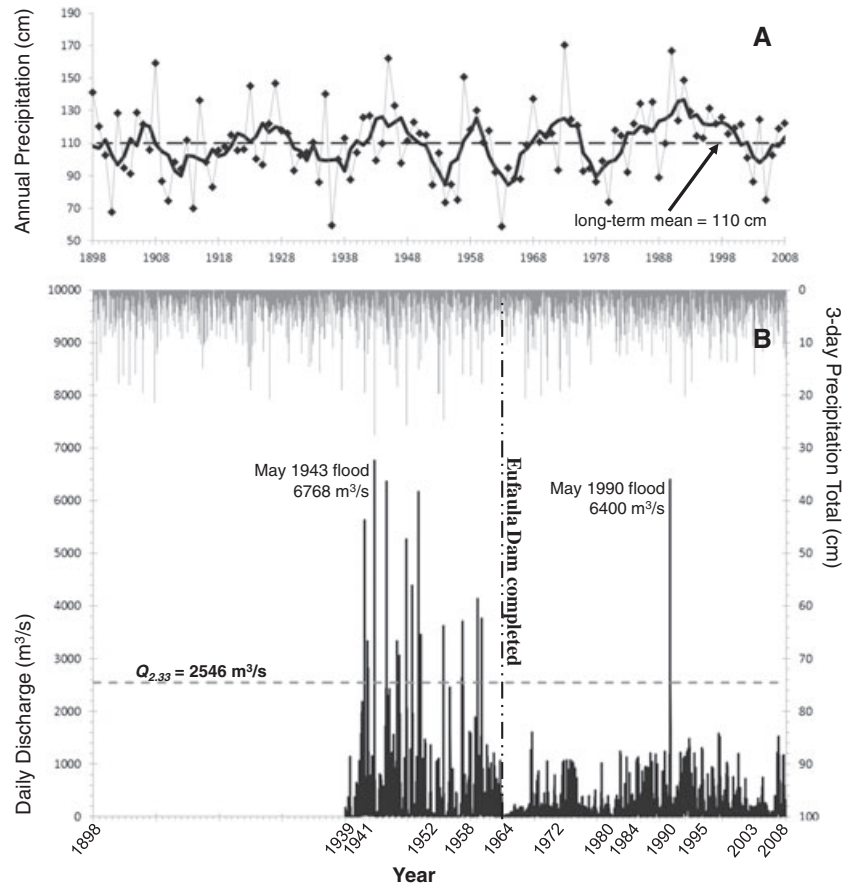
Figure 2. Precipitation and discharge time-series for the lower Canadian River (LCR), 1898–2008. Annual precipitation (black diamonds) with five-year mean (solid black line) is displayed on top (A). The dashed line at 110 cm is the long-term mean annual precipitation. Notice the approximate decadal cycle in wet (above dashed line) versus dry (below dashed line) periods as illustrated by the five-year mean precipitation. Daily discharge and three-day precipitation are displayed on bottom (B). Eufaula Dam was completed in 1964, with filling until 1967. The mean annual flood ($Q_{2.33}$) is represented by the dashed line. Year labels on bottom represent dates assessed for river channel and land cover changes.

NCDC, 2011). There was not a decreasing or increasing trend in precipitation, being statistically stationary throughout the 110 yr ($p > 0.10$). Additionally, there was not a temporal trend in the Q/P_{3d} time-series for 1938 to 1963 for either all runoff events ($p = 0.19$) or mean annual floods ($p = 0.92$), indicating that the relationship between rainfall and runoff remained statistically unchanged during this period despite land use changes throughout the watershed, mainly agriculture and urban development. We attribute their lack of impact on runoff to the high transmission losses in the upper and central portions of the watershed and the numerous flood-detention reservoirs constructed coincident with development.

Discharge (Q) displayed an irregular trend resulting from the construction of Eufaula Dam in 1964 (Figure 2). Before the dam, Q was highly variable with numerous low-flow periods ($< 4\,m^3/s$, 10th percentile) as long as weeks and massive floods as high as $6768\,m^3/s$. After dam completion, Q was much less variable with the greatest impact being the elimination of overbank floods. The one exception was in May 1990 when 40 cm of rain fell over two weeks during an already wet period, greatly exceeding the maximum storage capacity behind the dam.

Using the log-normal distribution, the mean annual 72-hour rainstorm ($P_{2.33}$) for 1938 to 1963 was 13.7 cm. The corresponding mean annual flood ($Q_{2.33}$) for this same period was $2546\,m^3/s$. From 1939 to 1964, there were 16 floods greater than $Q_{2.33}$, two every three years on average. After the dam was completed (1964–2008), our study reach only experienced the one flood in May 1990 described earlier, with an event peak of $6400\,m^3/s$. The next highest flood during this period was only $1597\,m^3/s$.

Land cover and soils

Land cover of the 79·39-km^2 LCRF also displayed an irregular temporal trend (Figure 3; Table I), one that was influenced by both agriculture and Eufaula Dam. In 1820, before European settlement in the region, LCRF was 'filled with close and entangled forests' (James, 1905, p. 176). Clearing of the LCRF began in the mid-nineteenth century and by 1898, 32% (25 km^2) of the floodplain had been converted to grassland/pasture and another 13% (10 km^2) had been devoted to cropland. Between 1898 and 1941, cropland more than doubled, mostly at the expense of forest. Then cropland decreased by 11% between 1941 and 1952, most of which was replaced by the new location of the active channel and successional forest. Cropland continued to decrease until 1964, when it covered only 9% of LCRF. At this time, the river (water and sand) occupied over 28% of the LCRF, almost twice as much as it did in 1898.

Following construction of the dam in 1964, the trend of land cover change reversed. Cropland increased, reaching a maximum of 40% in 1984. The active channel area decreased over this period, occupying only 16% of the LCRF in 1984. Post-dam changes in aerial extent of forest were minimal, especially after 1984 when it ranged 16–19%. From 1964 to 2008, grassland/pasture coverage fluctuated. In some years, it replaced inactive areas of river channel. Rotations between cropland and pasture also accounted for some of the fluctuation.

Soil composition varied widely across the LCRF, with silt-clay percentage (SC%) ranging 13–92% (Figure 4). The sandiest areas
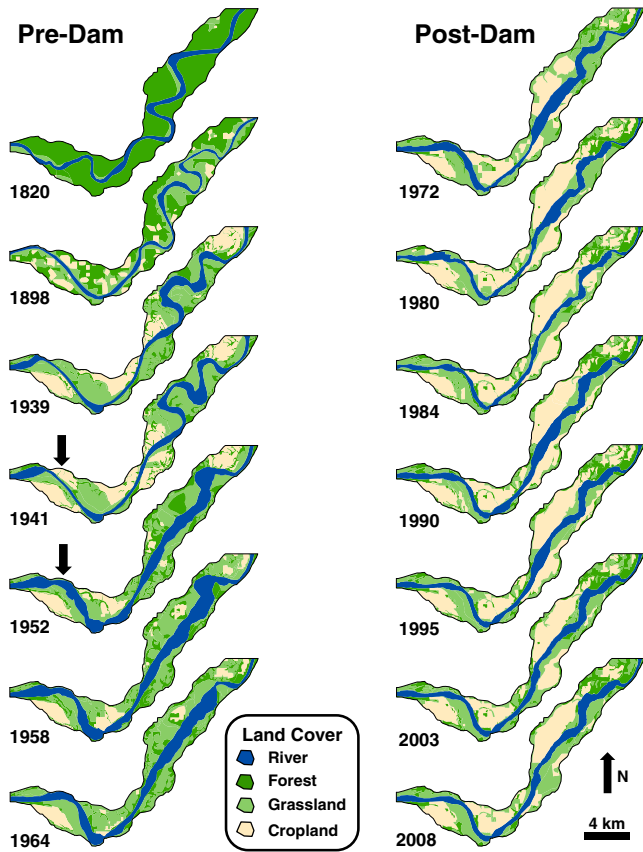
Figure 3. Land cover and channel changes in the lower Canadian River floodplain (LCRF) 1820–2008. Arrows in 1941 and 1952 illustrate one of the major croplands wiped out by channel widening and migration. This figure is available in colour online at wileyonlinelibrary.com/journal/espl

(~13 SC%) occurred along the channel margins. Prior channel locations also had relatively low SC% (Figures 3 and 4). Conversely, locations not occupied by river over the past 110 yr had the highest silt-clay content. These areas generally coincided with cultivated lands, where virtually all croplands were found in areas with greater than 22 SC%. There were only two areas of persistent cropland: the southwest and northwest corners, which coincided with the two highest elevations within the floodplain. These two areas were not flooded at any time during our study period, and with the recent channel incision we observed during field trips, have likely become abandoned floodplain.

Channel geometry and specific stream power (ω)

The lower Canadian River has meandered and migrated across most of its 2786 m wide floodplain over the past thousand or so years, as evidenced by former channel locations and meander scars. The only areas without evidence of former channels are the two elevated regions mentioned earlier. According to James (1905, p. 176), the mean channel width of our study reach in 1820 was somewhere between 300 and 400 m. In 1898, the active channel of the LCR occupied 11·6 km^2 with a mean width of 283 m (Figure 3, Table I). The meandering channel had a sinuosity of 1·44 and a slope of 0·00024. Between 1898 and 1964, the LCR cut off most of its meanders and straightened, eventually becoming a straight channel with a sinuosity of 1·17. Consequently, channel slope increased over this period, reaching 0·00030 in 1964. After the dam was constructed, channel slope and sinuosity remained at these values with minimal variability.

Mean active channel width (w_{ac}) more than doubled (283–759 m) between 1898 and 1958, followed by a decrease of 85 m in 1964. After dam completion in 1964, the channel narrowed considerably and rapidly, by 300 m in just 20 yr. The May 1990 flood widened the channel by 184 m. Over the next 18 yr, the channel gradually narrowed, with an w_{ac} of 509 m in 2008.

The changes in channel slope and width caused considerable changes in specific stream power for the same discharge. For example, the $Q_{2.33}$ of 2546 m^3/s in 1898 had a ω of 21·2 W/m^2. For this same Q in 1958, the increased w_{ac} resulted in a ω of 9·5 W/m^2. The channel narrowing over the next 32 yr increased potential ω considerably. There was not a discharge greater than 1597 m^3/s between August 1963 and April 1990; however, when the May 1990 flood occurred, the active channel was at its narrowest (374 m) since 1898, resulting in the highest single-event ω (48·6 W/m^2) over our entire record, despite it not being the highest Q. The channel widening from this flood caused a subsequent decrease in potential ω, followed by a gradual increase as the active channel narrowed through 2008.

There were reasonable relationships between channel widening and all four ω properties of event peak, magnitude, duration, and variability (Figure 5). However, the best predictor of channel widening, and the only significant one ($p = 0.033$), was magnitude of ω, with an r^2 of 0·82. A portion of the variability in this relationship was likely due to differences in riparian land cover among the measured intervals (i.e. non-forested banks are less resistant to erosion). If we account for this resistance by normalizing magnitude of ω (i.e. divide) by proportion of forest coverage, r^2 improves to 0·89. If magnitude of ω is log-transformed, r^2 improves to 0·94 ($p = 0.007$), or 0·97 ($p = 0.002$) if also normalized by forest coverage. Generally, the active channel widened when ω exceeded 10 W/m^2 for several days at a time and narrowed when this magnitude was not exceeded (Table I, Figure 6). The greatest amount of channel widening occurred during a period (1941–1952) when both magnitude of ω and floodplain cropland coverage (pre-dam) were at their highest.

Discussion and Conclusions

Influence of stream power and land cover on channel widening

The width of a river is determined by force–resistance relationships, and thus specific stream power (ω) and floodplain land cover both affected channel widening on the LCR. The magnitude of ω, which takes into account both its peak and duration, was likely the dominant influence on channel widening (Figure 5). In a study that took place approximately 300 km upstream of ours, Curtis and Whitney (2003) also found that magnitude of ω best explained erosion rates along the Canadian River. These findings support the conclusion of Julian and Torres (2006) that flood magnitude is the best predictor of erosion rates for channel banks composed of mostly non-cohesive sediment. Costa and O'Connor (1995) also employed this metric to define the most 'geomorphically effective flood,' using the term total energy expenditure per unit boundary area above some threshold. In rivers with high discharge variability such as the Canadian River, it is difficult to assign this 'dominant' discharge threshold (Pickup and Rieger, 1979); however, Figure 5(event peak) suggests that our use of the mean annual flood ($Q_{2.33}$) was not far off.

Characterizing the resistance of channel banks is a much more difficult task, especially in large floodplain-river systems

Table I. Timeline of changes in land cover, specific stream power, and channel geometry. River includes water and sand, which are grouped to represent the active channel and nullify changes caused by different river water levels. Floodplain area is 79·39 km² and valley length is 28·50 km. The mean annual flood ($Q_{2\cdot33}$) was 2546 m³/s.

Date (YYYY-MM-DD)	Land cover	Specific stream power (ω) -Number of floods $> Q_{2\cdot33}$ since prior date -Days that $Q > Q_{2\cdot33}$ -Maximum ω (Q) -$\Sigma \omega$ when $Q > Q_{2\cdot33}$	Channel geometry -Active channel area -Mean width -Channel slope (m/m) -Sinuosity (km/km)
Pre-Dam 1898-10-31	14·6 % River 40·7 % Forest 31·7 % Grassland 13·0 % Cropland		11·61 km² 283 m 0·00024 1·44
1939-08-21	21·0 % River 19·0 % Forest 38·2 % Grassland 21·8 % Cropland		16·67 km² 438 m 0·00026 1·34
1941-11-15	23·0 % River 16·5 % Forest 33·8 % Grassland 26·7 % Cropland	1 4 days 32·8 W/m² (5635 m³/s) 90·1 W/m²	18·26 km² 456 m 0·00025 1·40
1952-08-15	31·0 % River 20·9 % Forest 32·1 % Grassland 16·0 % Cropland	9 29 days 36·4 W/m² (6768 m³/s) 623·7 W/m²	24·65 km² 722 m 0·00029 1·20
1958-06-24	32·9 % River 20·0 % Forest 35·6 % Grassland 11·5 % Cropland	4 10 days 14·6 W/m² (3710 m³/s) 120·8 W/m²	26·08 km² 759 m 0·00029 1·21
1964-11-20	28·3 % River 19·5 % Forest 43·0 % Grassland 9·2 % Cropland	2 6 days 15·5 W/m² (4134 m³/s) 81·6 W/m²	22·48 km² 674 m 0·00030 1·17
Post-Dam 1972-04-01	23·6 % River 12·2 % Forest 36·6 % Grassland 27·6 % Cropland	0 0 7·0 W/m² (1597 m³/s) 0	18·71 km² 549 m 0·00029 1·19
1980-04-20	19·8 % River 14·0 % Forest 27·0 % Grassland 39·2 % Cropland	0 0 5·5 W/m² (1070 m³/s) 0	15·72 km² 464 m 0·00029 1·19
1984-07-22	15·9 % River 16·7 % Forest 27·2 % Grassland 40·2 % Cropland	0 0 7·6 W/m² (1243 m³/s) 0	12·65 km² 374 m 0·00029 1·19
1990-12-18	23·5 % River 16·7 % Forest 21·2 % Grassland 38·6 % Cropland	1 8 d 48·6 W/m² (6400 m³/s) 286·6 W/m²	18·64 km² 558 m 0·00030 1·17
1995-03-09	21·7 % River 16·1 % Forest 25·0 % Grassland 37·2 % Cropland	0 0 7·8 W/m² (1484 m³/s) 0	17·25 km² 516 m 0·00030 1·17
2003-09-26	20·7 % River 18·8 % Forest 26·1 % Grassland 34·4 % Cropland	0 0 9·0 W/m² (1583 m³/s) 0	16·41 km² 490 m 0·00030 1·17
2008-06-27	21·4 % River 15·9 % Forest 30·9 % Grassland 31·8 % Cropland	0 0 9·2 W/m² (1529 m³/s) 0	17·02 km² 509 m 0·00030 1·17

(Schumm and Lichty, 1963; Costa and O'Connor, 1995). In Schumm and Lichty's (1963) study of the Cimarron River, a Great Plains river much like the Canadian River, they concluded that riparian vegetation played a major role in dictating channel width, with forested banks being much more resistant to widening. While they did not establish a clear relationship between floodplain agriculture and erosion rates, Schumm and Lichty did find that the greatest widening occurred during a period of major agricultural activity. Like their study, the temporal resolution of our study prevented us from providing stronger evidence for the effects of floodplain agriculture on channel erosion. Thus, we relied largely on visual evidence (Figure 3) and a long record of empirical trends (Figure 6) to infer the process-based relationships described later.
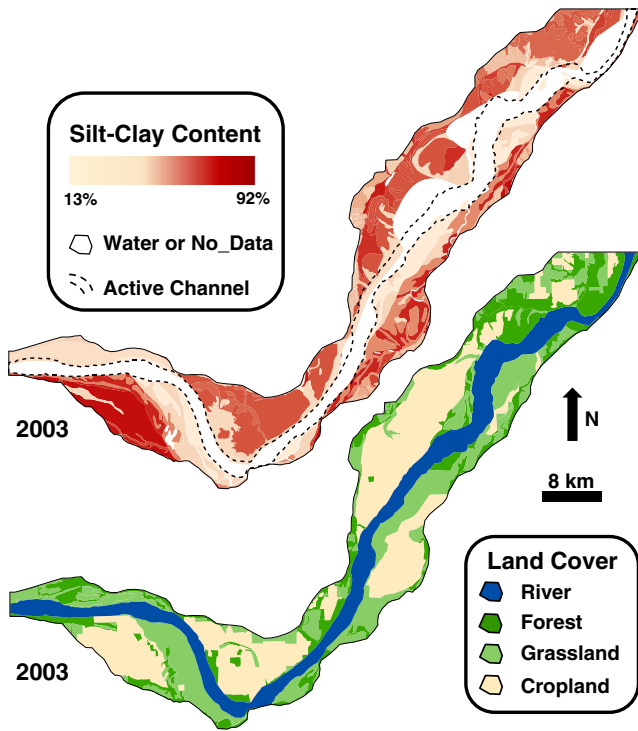
Figure 4. Soil composition (top) and land cover (bottom) of the lower Canadian River floodplain (LCRF) for 2003. Soil map derived from SSURGO data collected in 2003. The active channel for 2003 is shown for reference. Notice that croplands are generally located in areas where silt-clay content > 22%. Also note that sandy areas occur at former channel locations, by referencing Figure 3. This figure is available in colour online at wileyonlinelibrary.com/journal/espl

Feedbacks

The Canadian River has been characterized as 'one of the most dynamic and variable river environments anywhere in the world' (Hefley, 1937; Matthews *et al.*, 2005), resulting from having a floodplain-channel composed mostly of non-cohesive

sand that experiences extreme climate and flow variability (Osterkamp and Hedman, 1982; Williams and Wolman, 1984). The silty overbank deposits from these frequent floods made the LCRF particularly fertile. However, several factors emerged from our pre-dam analyses that likely discouraged early peoples from cultivating this land: (i) periodic destructive flooding, mostly during early summer (Figure 2); (ii) frequent channel migration (Figure 3); and (iii) unfertile land of previous channel locations (Figure 4). Accordingly, the LCRF remained essentially undeveloped through 1820 despite an agricultural presence in the region (James, 1905; Figure 3).

The LCRF eventually became cultivated in the mid-nineteenth century and by 1898, 45% of the previously forested floodplain had been converted to either cropland or pasture. Cropland, in particular, continued to increase and by 1941 had more than doubled to 27% (Figure 6). After 1941, cropland declined rapidly, reaching a minimum of 9% in 1964. While the temporal trends in floodplain cultivation largely followed those of the surrounding region (Figure 6), there were some deviations. For example, regional cropland areas increased in 1949 and again in 1959, yet continued to decrease rapidly in the floodplain. We attribute these declines in floodplain cultivation to two related factors: the above-average magnitude of floods 1940–1951 and 1957–1961 in East-Central Oklahoma and loss of cropland to active channel. As the arrows in Figure 3 illustrate, one of the largest cultivated fields in 1941 was completely wiped out and replaced with active channel by 1952. Large areas of cropland in the central and eastern floodplain were also wiped out during this period. These losses, both spatially and economically, made the farmers appreciate the inherent risk of floodplain agriculture and likely discouraged them from cultivating new areas in the LCRF. Further, the land of the former channel location, now mostly sterile sand, would take many decades to accumulate enough silt, clay, and organic matter to become fertile enough for cultivation (Dort, 2009). Our results showed that only areas with greater than 22% silt-clay content sustained croplands (Figure 4).

While any area of the floodplain is susceptible to fluvial erosion, non-forested areas are more erodible than forested areas
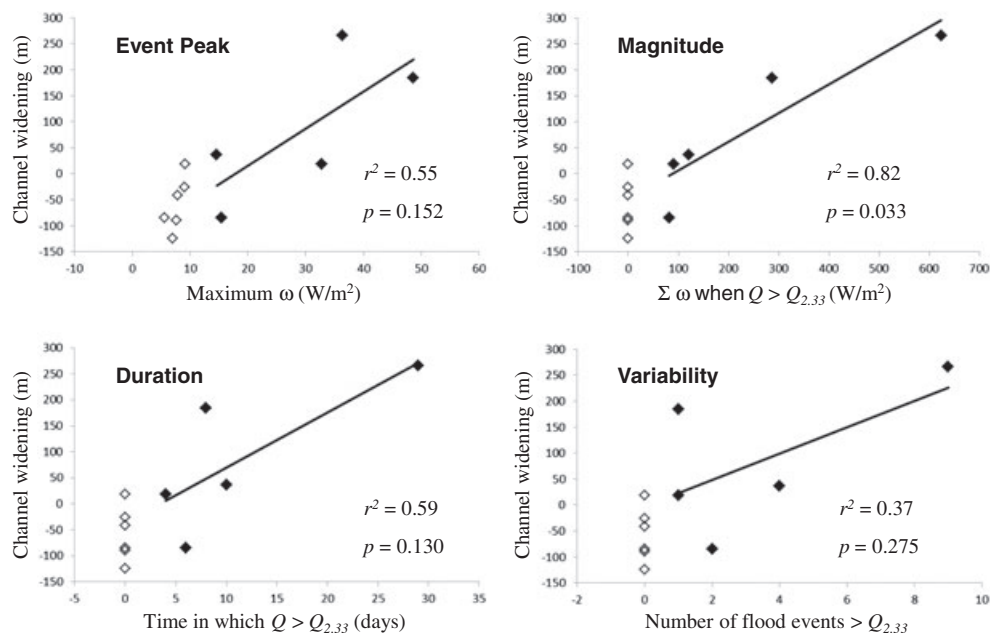

Figure 5. Relationships between channel widening and the specific stream power (ω) properties of event peak, magnitude, duration, and variability. In order to have an equal sample size for all four properties, only intervals with an active channel flood ($Q_{2.33}$) were used for regression analysis (closed diamonds). Intervals without a mean annual flood are denoted by open diamonds. Negative values of channel widening represent channel narrowing.
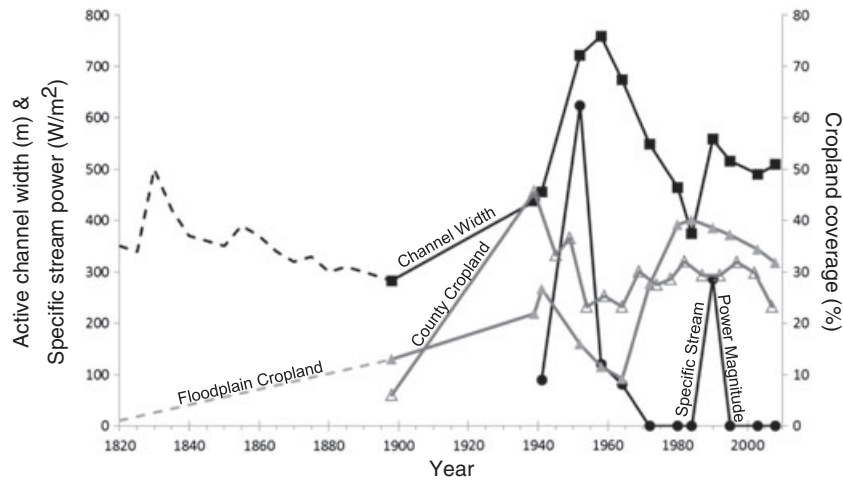
Figure 6. Historical range of variability in county cropland coverage (open triangles), floodplain cropland coverage (closed triangles), active channel width (closed squares), and magnitude of specific stream power (closed circles; sum of all events greater than the mean annual flood during that period) in the lower Canadian River. Values before 1898 (dashed lines) are estimated from the historical account of James (1905), with assumed year-to-year variability in channel width and no assumption with respect to cropland trend. Alternating trends in floodplain cropland coverage, channel width, and specific stream power reveal feedbacks among the three variables.

because of less surface roughness and less soil strength (Micheli *et al.*, 2004; Thorne, 1990). The channel changes we observed from 1898 to 1964 support this trend where agricultural areas, especially croplands, were most vulnerable to channel widening and meander cutoffs (Figure 3). The rapid increase in cropland from 1898 to 1941 therefore created a negative feedback where more erosion from more croplands led to increases in active channel area, which resulted in decreases in cropland area after 1941 (Figure 6). This process led to another negative feedback where less land clearing/usage and a wider channel reduced potential ω and promoted vegetation colonization of the channel margins, resulting in channel narrowing beginning in 1958. This channel narrowing, along with the now steeper channel slope, gradually increased potential ω.

This alternating cycle of channel narrowing and widening would have continued, as it likely had for thousands of years; however, the construction of Eufaula Dam in 1964 disrupted this feedback loop. In addition to hydropower, one of the purposes of the dam was to eliminate overbank floods ($> Q_{2.33}$). Without enough specific stream power for erosion of the active channel, a positive feedback ensued where inactive channel margins allowed encroachment by floodplain vegetation which promoted sediment deposition and thus more colonization, with the end result being continued channel narrowing (Figure 6). Another positive feedback initiated by the dam is that by blocking bedload sediment to the downstream reach, the channel incised (~1 m reach-averaged as of 1977; Williams and Wolman, 1984), which further reduced the possibility of overbank flooding. The reduced threat of flooding resulted in a resurgence of floodplain cultivation, which more than quadrupled in just 20 yr following dam completion. Conversely, the lack of overbank floods initiates a negative feedback with cultivation, or at least limits its extent. Without overbank floods, the supply of silty deposits that maintain the floodplain's fertility are shut off. This process could explain why post-dam cropland area has been declining since 1984, despite general increases in regional cropland area to 1997 (Figure 6). Another possible explanation is that farmers became cautious after the devastating May 1990 flood, which showed them a dam cannot prevent all floods.

When the 1990 flood occurred, the LCR channel was at its narrowest since 1898 and half of what it was in 1958. This narrow width, together with the steeper channel slope, produced the highest single-event ω on record for LCR, with $Q_{2.33}$ being

exceeded for an unprecedented eight consecutive days. This exceptionally high magnitude of ω caused extensive channel widening, especially in non-forested agricultural areas (Figure 3). Following some initial channel narrowing from vegetation encroachment, the LCR has maintained a relatively constant width of 500 m, which we and others attribute to the high daily ramping rates in discharge (namely power-peaking) from hydropower releases (Williams and Wolman, 1984). These high discharge releases scour channel bars on an almost daily
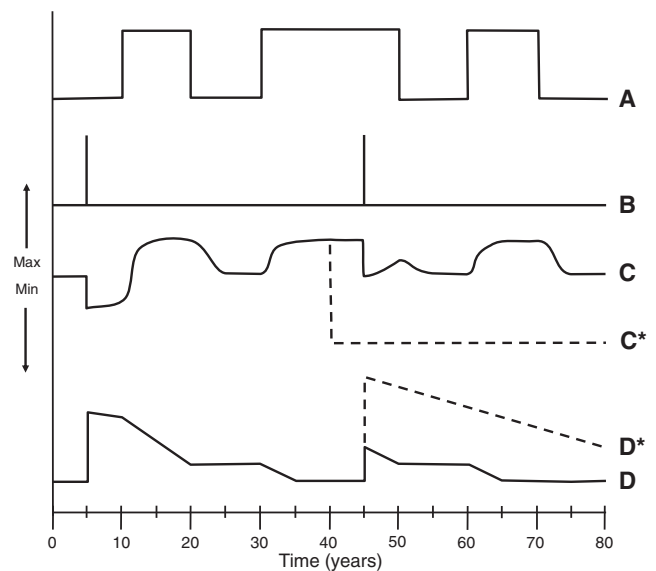

Figure 7. Biogeomorphic response model of floodplain forest cover (C) and active channel width (D) of large Great Plains rivers in response to variable precipitation (A) and large floods (40-yr return period in this case; B). Precipitation (wet versus dry period) and floods are independent variables, and are independent of one another. Active channel width and floodplain forest cover are dependent variables and are dependent on each other through feedbacks; where increases in channel width from floods remove floodplain forests, and re-growth of floodplain forests, especially during wet periods, reduce channel width. C* and D* (dashed lines) represent a scenario in which all floodplain forests were cleared for agriculture in year 40. Model was based on the concept of Knox's (1972) biogeomorphic response model, but used data and patterns from this study among many others (see text).

basis, which prevents vegetation establishment and consequent channel narrowing. This dam-induced impedance to floodplain vegetation colonization can also have feedbacks on channel geometry, especially width and sinuosity (Camporeale and Ridolfi, 2010; Tealdi *et al.*, 2011). These changes in channel morphology and hydrology likely have altered forest species composition throughout the LCRF as well (Johnson, 1992).

Biogeomorphic response model of large Great Plains rivers

Effects of hydrologic regime on vegetation and channel geometry are well documented (Knox, 1972), where increased precipitation generally leads to increased vegetation and consequently less geomorphic work. Although Knox's (1972) biogeomorphic response model is used to characterize sediment yield at the watershed scale, it can be used just as effectively, with appropriate modifications, to model changes in active channel width at the floodplain scale (Figure 7). Precipitation in the Great Plains generally has decadal (or bidecadal) cycles of alternating wet and dry periods (Figures 2 and 7A). Floodplain vegetation usually follows this trend with forest expansion during wetter periods and forest contraction during drier periods (Figure 7C; Schumm and Lichty, 1963; Martin and Johnson, 1987). While floodplain forests tend to be more resilient to drought than upland forests, they are still susceptible to dieback during multi-year droughts, especially in sub-humid to semi-arid regions with warm summers (such as the Great Plains) where water tables can drop considerably due to prolonged periods of low precipitation and high evapotranspiration rates. Increased anthropogenic water extractions during droughts compound this problem (Horner *et al.*, 2009).

Large floods are also a common phenomenon in Great Plains rivers; however, they are independent of decadal precipitation trends (Figure 2; Schumm and Lichty, 1963). For example, the 40-yr flood can occur during a dry or wet period (the first and second floods in Figure 7B, respectively). These large floods are particularly destructive on the mostly non-cohesive boundary materials of large Great Plains rivers (Dort, 2009), widening the channel considerably through bank erosion (Figure 7D) and removing large areas of floodplain forest (Figure 7C). The amount of channel widening is inversely related to riparian forest cover (Micheli *et al.*, 2004; VanLooy and Martin, 2005; but see Burkham, 1972). Following the erosion event, the active river channel begins to narrow, with the rate of narrowing dependent on the variability of sediment erosional/depositional events and rate of encroachment by floodplain vegetation (Burkham, 1972; Friedman *et al.*, 1996; Miller and Friedman, 2009). In the absence of another large destructive flood, the channel will begin to narrow relatively rapidly within the next few years subsequent to the flood due to reduced specific stream power, and then relatively slowly as it approaches its pre-flood width (Figure 7D; Friedman *et al.*, 1996; VanLooy and Martin, 2005). Previous studies indicate that it may take 40 yr for these large sand-bed rivers with cottonwood-willow riparian forests to return to their pre-flood width (Burkham, 1972; Curtis and Whitney, 2003; VanLooy and Martin, 2005).

An important component of our biogeomorphic response model is that it incorporates feedbacks between riparian vegetation and channel width. Riparian forest cover will be influenced by changes in channel width, and channel width will be inversely related to riparian forest cover. If the riparian forest is removed, such as for agriculture (Figure 7C*), subsequent large floods will result in extraordinary channel widening (Figure 7D*) due to the decreased resistance of non-forested banks. With less riparian forest for encroachment, channel narrowing will occur

at a slower rate. All of these changes in channel width will have feedbacks on specific stream power, which are not depicted in Figure 7, but can be seen in Figure 6. These changes in ω, in turn, have feedbacks on riparian vegetation and channel width. Agriculture is the only anthropogenic disturbance depicted in our simplified biogeomorphic response model; however, others such as water diversions, upstream dams, and exotic vegetation could also be incorporated.

Historical range of variability

In characterizing the historical range of variability of the LCRF, we segregate it into three periods: pre-dam/pre-agriculture (*c.* 500–1820), pre-dam/post-agriculture (1898–1964), and post-dam/post-agriculture (1964–present). Before the dam and floodplain agriculture, the LCR was a meandering river with a sinuosity that varied about 1·5 and exhibited a braided pattern at low flows. Because of the frequent and sometimes long droughts that occur in the region, the reach alternated between periods of aggradation and degradation (Curtis and Whitney, 2003). Accordingly, channel slope would have also varied, but remained low (0·00024 in 1898). Active channel width varied along the reach, but likely did not exceed 400 m for any long period of time given its relatively narrow valley compared to upstream reaches and the rapid colonization by the dense floodplain forests following destructive floods (James, 1905; Hefley, 1937). Based on meander scar locations, the active channel migrated across most of the floodplain during these 1300 yr. Using this channel geometry and historical discharge records, maximum ω likely varied between 10 and 60 W/m^2 (Nanson and Croke, 1992).

When most of the LCRF was cleared for agriculture, stream power, channel geometry, and land cover all changed. Between 1898 and 1964, grassland/pasture varied 31–43% and cropland varied 9–27%. The LCR straightened considerably during this time. By the end of this period, sinuosity had decreased to 1·17 and channel slope had increased to 0·00030. The less stable banks resulted in a much wider channel that varied from 438 to 759 m. This wider channel lowered ω, whose maximum was 38 W/m^2 but rarely exceeded 15 W/m^2.

The major consequence of Eufaula Dam on the LCRF was the virtual elimination of overbank floods ($> Q_{2.33}$). Without active channel floods, the channel became static, particularly with respect to channel slope, sinuosity, and migration. Active channel width did vary (374–549 m), but with the absence of any overbank floods for the past 20 yr, the channel has become relatively stable with a width of 500 m. Other than the one flood in 1990, ω never exceeded 10 W/m^2. Under this flow regime and using the classification of Nanson and Croke (1992), the LCRF is no longer a dynamic river-floodplain system.

References

Anderson JR, Hardy EE, Roach JT, Witmer RE. 1976. *A Land Use and Land Cover Classification System for Use with Remote Sensor Data*, Geological Survey Professional Paper 964. US Government Printing Office: Washington, DC.

Burkham DE. 1972. *Channel Changes of the Gila River in Safford Valley, Arizona, 1846–1970*, US Geological Survey Professional Paper 655-G. US Geological Survey: Reston, VA; 1–24.

Camporeale C, Ridolfi L. 2010. Interplay among river meandering, discharge stochasticity and riparian vegetation. *Journal of Hydrology* **382**: 138–144. DOI. 10.1016/j.jhydrol.2009.12.024

Costa JE, O'Connor JE. 1995. Geomorphically effective floods. In *Natural and Anthropogenic Influences in Fluvial Geomorphology*, Costa JE, Miller AJ, Potter KW, Wilcock PR. American Geophysical Union: Washington, DC.

Costanza R, dArge R, deGroot R, Farber S, Grasso M, Hannon B, Limburg K, Naeem S, Oneill RV, Paruelo J, Raskin RG, Sutton P, vandenBelt M. 1997. The value of the world's ecosystem services and natural capital. *Nature* **387**: 253–260.

Curtis JA, Whitney JW. 2003. Geomorphic and hydrologic assessment of erosion hazards at the Norman municipal landfill, Canadian River floodplain central Oklahoma. *Environmental and Engineering Geoscience* **9**: 241–252.

Dort W Jr. 2009. *Historical Channel Changes of the Kansas River and its Major Tributaries*, American Geographical Society, Special Publication 42. American Geographical Society: New York; 80 pp.

Friedman JM, Osterkamp WR, Lewis WM. 1996. The role of vegetation and bed-level fluctuations in the process of channel narrowing. *Geomorphology* **14**: 341–351.

Friedman JM, Osterkamp WR, Scott ML, Auble GT. 1998. Downstream effects of dams on channel geometry and bottomland vegetation: regional patterns in the Great Plains. *Wetlands* **18**: 619–633.

Graf WL. 2001. Damage control: restoring the physical integrity of America's rivers. *Annals of the Association of American Geographers* **91**: 1–27.

Gregory SV, Swanson FJ, McKee WA, Cummins KW. 1991. An ecosystem perspective of riparian zones. *Bioscience* **41**: 540–551.

Hefley HM. 1937. Ecological studies on the Canadian River floodplain in Cleveland County, Oklahoma. *Ecological Monographs* **7**: 345–402.

Hoagland B. 2000. The vegetation of Oklahoma: a classification for landscape mapping and conservation planning. *The Southwestern Naturalist* **45**: 385–420.

Hooke JM. 1979. An analysis of the processes of river bank erosion. *Journal of Hydrology* **42**: 39–62.

Horner GJ, Baker PJ, MacNally R, Cunningham SC, Thomson JR, Hamilton F. 2009. Mortality of developing floodplain forests subjected to a drying climate and water extraction. *Global Change Biology* **15**: 2176–2186.

Hupp CR, Osterkamp WR. 1996. Riparian vegetation and fluvial geomorphic processes. *Geomorphology* **14**: 277–295.

James E. 1905. *James's Account of S. H. Long's Expedition, 1819–1820.* A.H. Clark: Cleveland, OH.

Joeckel RM, Henebry GM. 2008. Channel and island change in the lower Platte River, Eastern Nebraska, USA: 1855–2005. *Geomorphology* **102**: 407–418.

Johnson WC. 1992. Dams and riparian forests: case study from the upper Missouri River. *Rivers* **3**: 229–242.

Jones KB, Slonecker ET, Nash MS, Neale AC, Wade TG, Hamann S. 2010. Riparian habitat changes across the continental United States (1972–2003) and potential implications for sustaining ecosystem services. *Landscape Ecology* **25**: 1261–1275.

Julian JP, Torres R. 2006. Hydraulic erosion of cohesive riverbanks. *Geomorphology* **76**: 193–206.

Junk WJ, Bayley PB, Sparks RE. 1989. The flood pulse concept in river-floodplain systems. In *Proceedings of the International Large River Symposium*, Dodge DP (ed.), Canadian Special Publication. Fisheries and Aquatic Science **106**: 110–127.

Knox JC. 1972. Valley alluviation in southwestern Wisconsin. *Annals of the Association of American Geographers* **62**: 401–410.

Martin CW, Johnson WC. 1987. Historical channel narrowing and riparian vegetation expansion in the Medicine Lodge River Basin, Kansas, 1871–1983. *Annals of the Association of American Geographers* **77**: 436–449.

Matthews WJ, Vaughn CC, Gido KB, Marsh-Matthews E. 2005. Southern Plains rivers. In *Rivers of North America*, Benke AC, Cushing CE (eds). Academic Press: Burlington; 283–325.

Micheli ER, Kirchner JW, Larsen EW. 2004. Quantifying the effect of riparian forest versus agricultural vegetation on river meander migration rates, Central Sacramento River, California, USA. *River Research and Applications* **20**: 537–548.

Miller JR, Friedman JM. 2009. Influence of flow variability on floodplain formation and destruction, Little Missouri River, North Dakota. *GSA Bulletin* **121**: 752–759.

Nanson GC, Croke JC. 1992. A genetic classification of floodplains. *Geomorphology* **4**: 459–486.

National Climatic Data Center (NCDC). 2011. *Climate Division Temperature–Precipitation–Drought Data*. NCDC: East-Central, OK.

Osterkamp WR, Hedman ER. 1977. Variation of width and discharge for natural high-gradient stream channels. *Water Resources Research* **13**: 256–258.

Osterkamp WR, Hedman ER. 1982. *Perennial-streamflow Characteristics Related to Channel Geometry and Sediment in Missouri River Basin*, USGS Professional Paper 1242. US Geological Survey: Reston, VA; 1–37.

Pickup G, Rieger WA. 1979. A conceptual model of the relationship between channel characteristics and discharge. *Earth Surface Processes* **4**: 37–42.

Schulte LA, Mladenoff DJ. 2001. The original U.S. Public Land Survey Records: their use and limitations in reconstructing presettlement vegetation. *Journal of Forestry* **99**: 5–10.

Schumm SA, Lichty RW. 1963. *Channel widening and flood-plain construction along Cimarron River in southwestern Kansas*, Geological Survey Professional Paper 352-D. US Geological Survey: Washington, DC; 18 pp.

Schumm SA, Lichty RW. 1965. Time, space, and causality in geomorphology. *American Journal of Science* **263**: 110–119.

Tealdi S, Camporeale C, Ridolfi L. 2011. Modeling the impact of river damming on riparian vegetation. *Journal of Hydrology* **396**: 302–312. DOI. 10.1016/j.jhydrol.2010.11.016

Thorne CR. 1982. Processes and mechanisms of river bank erosion. In *Gravel-bed Rivers*, Hey RD, Bathurst JC, Thorne CR (eds). John Wiley & Sons: London.

Thorne CR. 1990. Effects of vegetation on riverbank erosion and stability. In *Vegetation and Erosion*, Thornes JB (ed.). John Wiley & Sons: Chichester; 125–144.

Tockner K, Stanford JA. 2002. Riverine flood plains: present state and future trends. *Environmental Conservation* **29**: 308–330.

VanLooy JA, Martin CW. 2005. Channel and vegetation change on the Cimarron River, southwestern Kansas, 1953–2001. *Annals of the Association of American Geographers* **95**: 727–739.

Ware GH, Penfound WT. 1949. The vegetation of the lower levels of the floodplain of the south Canadian River in central Oklahoma. *Ecology* **30**: 478–484.

Watkins BW. 2007. Reconstructing the Choctaw Nation of Oklahoma, 1894–1898: Landscape and Settlement on the Eve of Allotment, PhD Thesis, Oklahoma State University; 202.

Whitney GG, DeCant JP. 2001. Government land office surveys and other early land surveys. In *The Historical Ecology Handbook: A Restorationist's Guide to Reference Ecosystems*, Egan D, Howell EA (eds). Island Press: Washington, DC; 147–172.

Williams GP, Wolman MG. 1984. *Downstream Effects of Dams on Alluvial Rivers*. USGS Professional Paper 1286. US Geological Survey: Reston, VA; 83.

Zaimes GN, Schultz RC, Isenhart TM. 2004. Stream bank erosion adjacent to riparian forest buffers, row-crop fields, and continuously-grazed pastures along Bear Creek in central Iowa. *Journal of Soil and Water Conservation* **59**: 19–27.